NMR relaxometry: Spin lattice relaxation times in the laboratory frame versus spin lattice relaxation times in the rotating frame

Emilie Steiner, Mehdi Yemloul, Laouès Guendouz, Sébastien Leclerc, Anthony Robert, Daniel Canet

NMR relaxometry : spin lattice relaxation times in the laboratory frame versus spin lattice relaxation times in the rotating frame

Emilie Steiner[1], *Mehdi Yemloul*[1], *Laouès Guendouz*[2], *Sébastien Leclerc*[3], *Anthony Robert*[1], *Daniel Canet*[1*]

[1]Méthodologie RMN (CRM2, UMR 7036 CNRS- Nancy-Université),
Faculté des Sciences et Technologies, BP 70239
54506 Vandoeuvre-lès-Nancy Cedex (France)

[2]Laboratoire d'Instrumentation Electronique de Nancy (EA 3440)
Faculté des Sciences et Technologies BP 70239
54506 Vandoeuvre-lès-Nancy (cedex), France

[3]LEMTA (UMR 7563 CNRS- Nancy-Université), BP 160, 54504 Vandoeuvre-lès-Nancy (cedex), France

*Corresponding author: Daniel.Canet@crm2.uhp-nancy.fr

Abstract

Relaxometry dispersion curves display the spin lattice relaxation rate as a function of the measurement frequency. However, as far as proton NMR is considered, dispersion curves usually start around 5 kHz and thus miss the very low frequency region. This gap can be filled by the measurement of the spin-lattice relaxation rate in the rotating frame. The issue of connecting both relaxation rates is considered for two relaxation mechanisms: i) randomly varying magnetic fields, ii) dipolar interaction within a system of two equivalent spins. Appropriate data processing is presented and the random field mechanism turns out to be adequate.

1. Introduction

Measurement and interpretation of NMR relaxation times as a function of the measurement frequency ω_0 (or, equivalently, as a function of the NMR static magnetic field B_0 through the Larmor equation $\omega_0 = \gamma B_0$, γ being the gyromagnetic ratio of the considered nucleus) is called relaxometry. Applications are numerous [1] ranging from the characterization of slow molecular motions in complex systems to the effects of paramagnetic species on biological fluids. Dedicated instruments, called relaxometers (working according to field cycling methodology), are available in a range going from some kHz (say 5 kHz) to some tens of MHz (typically from 10 MHz to 40 MHz). Higher frequencies can be investigated with conventional NMR spectrometers, possibly with variable field electromagnets in the range 10 MHz-100 MHz, or at still higher frequencies with fixed frequency cryomagnets. Results, in terms of the longitudinal relaxation rate R_1 (the inverse of the relaxation time T_1), are usually presented in the form of a so-called dispersion curve, R_1 being the ordinate (with a logarithmic scale if variations are important) and the measurement frequency as abscissa (generally with a logarithmic scale). These dispersion curves present a gap in the frequency range going from zero frequency up to some tens of kHz. The present study is devoted to the way of filling this gap which can contain important information about slow motions or exchange phenomena. One possibility, explored in this paper, is to measure the so-called relaxation time in the rotating frame ($T_{1\rho}$ or its inverse $R_{1\rho}$) as a function of $\omega_1 = \gamma B_1$ where B_1 is the amplitude of the radio-frequency (rf) field along which nuclear magnetization is locked (measuring this relaxation time is accomplished by following the decay of locked magnetization). However, the major concern is that $R_{1\rho}$ does not depend on ω_1 in the same way as R_1 depends on ω_0 [2,3]. Indeed, in the case of diamagnetic systems, in only one instance [4] (to the best of our knowledge) was the $R_{1\rho}$ dispersion curve directly linked to the R_1 dispersion curve. It can

be mentioned that, in the case of paramagnetic relaxation enhancement (PRE), Fries et al. recently proposed [5] to use a linear combination of R_1 and $R_{1\rho}$. The approach presented here is along the same lines and could be applied to systems which possess a slow electronic spin relaxation [6], thus not overwhelming the low-frequency $R_{1\rho}$ dispersion. Otherwise $R_{1\rho}$ has been mostly used to characterize very slow motions [7, 8] or exchange phenomena in biological systems through ^{15}N [9-14] or proton [15] measurements. It must be noticed that, in order to increase the frequency range, off-resonance experiments, first introduced by Desvaux [16], were employed [8,11-15]. This adds however some complexity in the exploitation of experimental data.

The present work is devoted to a transformation of $R_{1\rho}$ data so that they can complement the R_1 dispersion curve toward the very low frequencies. Obtaining a full dispersion curve presents obviously some advantages in terms of the accuracy of parameters derived from dispersion curves and may reveal relaxation mechanisms undetectable at higher frequencies. Exchange phenomena will not be envisionned here. The proposed procedure will be considered theoretically and two examples will be given: one dealing with a solvent in interaction with the surface of an organogel, the protons of this solvent being subjected in addition to a constant contribution due to paramagnetic relaxation, the other with the different types of water in a mesoporous medium.

2. Theory

The expressions of the three relaxation rates we are concerned with here (the spin-lattice or longitudinal R_1, the spin-spin or transverse R_2, the spin-lattice in the rotating frame $R_{1\rho}$) depend obviously on the relaxation mechanisms. We shall be dealing exclusively with dipolar interactions experienced by the proton(s) of the molecules under investigation. Two situations can be envisioned: i) interactions arise from outside; in that case randomly fluctuating

magnetic fields constitute a good approximation for evaluating the spectral densities entering the expression of relaxation parameters; ii) interactions take place inside the set of the considered protons (e.g. the dipolar interaction between the two protons of the water molecule) and one has to take heed of the whole system (constituted of "like spins", according to Abragam's terminology [17]) and, as will be seen below, this entails some complications. Of course, the present treatment rests on the hypothesis of classical dipolar interactions and would probably need some modifications in the case of a quantum magnetic moment, e.g. a paramagnetic ion [18].

Equations given below are expressed in terms of spectral densities [19,20], their simplest form being

$$J(\omega) = \frac{2\tau_c}{1+\omega^2\tau_c^2} \qquad (1)$$

where τ_c is a correlation time describing a motion supposed isotropic. Of course, the expressions below can accommodate any type of spectral density.

Random fields

ω_0 and ω_0' being measurement frequencies, one has for the three relaxation rates

$$R_1(\omega_0) = C2J(\omega_0) + R^{other} \qquad (2)$$

$$R_2 = C[J(0) + J(\omega_0')] + R^{other} \qquad (3)$$

$$R_{1\rho}(\omega_1) = C[J(\omega_1) + J(\omega_0')] + R^{other} \qquad (4)$$

C stands for a factor including constants and the amplitude of the relevant dipolar interaction while R^{other} stands for the contribution of other relaxation mechanisms. ω_0 represents the low frequencies at which R_1 is measured, just above (or overlapping with) the frequency range covered by the $R_{1\rho}$ measurements. ω_0' is the frequency (relatively high for sensitivity

reasons) of the spectrometer with which these latter measurements have been carried out. (2) arises from the correlation function of the random field transverse components (*x* and *y*), hence the ω_0 dependency which corresponds to the precession of the two homolog magnetization components. Conversely, (3) and (4) depend on one transverse component and of the longitudinal component (*z*). The latter is responsible for the spectral density at zero frequency (no precession) in (3) and at ω_1 (nutation around the rf field) in (4). It can be noticed that the only difference between $R_{1\rho}$ and R_2 is the substitution of $J(0)$ by $J(\omega_1)$.

From equations (2) and (4), it is obvious that, in non extreme narrowing conditions, $R_{1\rho}(\omega)$ cannot be equal to $R_1(\omega)$. $R_{1\rho}(\omega)$ can however be processed according to the following algebra. Consider the frequency ω_{1b} in the region where $R_{1\rho}$ and R_1 overlap. We can always write

$$2R_{1\rho}(\omega_{1b}) = 2CJ(\omega_{1b}) + R^{other} + C' \qquad (5)$$

with the *constant* C' defined as

$$C' = 2R_{1\rho}(\omega_{1b}) - R_1(\omega_{1b}) = 2CJ(\omega_0^{'}) + R^{other} \qquad (6)$$

Consider now a frequency ω_{1a} where only $R_{1\rho}$ is available. In order to compare and eventually to connect R_1 and $R_{1\rho}$ data, the latter must be substituted by $R_{1\rho}^{'}$ which we define as

$$R_{1\rho}^{'}(\omega_{1a}) = 2R_{1\rho}(\omega_{1a}) - C' \qquad (7)$$

$R_{1\rho}^{'}(\omega_{1a})$ should therefore be identical to $R_1(\omega_{1a})$.

Measurements of $R_{1\rho}$ are performed for different values of ω_1 (by varying the amplitude of the rf field). According to equation (7), they are then multiplied by two and subtracted by a quantity independent of ω_1 and corresponding to $2J(\omega_0^{'})$ and to other contributions to the relaxation rates, constant at these low frequencies. In practice, this quantity is determined by

making coincident, in the overlap region, the two dispersion curves $R_1(\omega_0)$ and $R_{1\rho}(\omega_1)$. Of course, the rf field amplitude cannot be made infinitely small. Fortunately, $J(0)$ is better deduced from the measurement of R_2 to which the above treatment can be applied as well.

Like spins

With the same notations as in the previous section, one has [2,3,17,19,20]

$$R_1 = C[4J(2\omega_0) + J(\omega_0)] + R^{other} \approx 5CJ(\sqrt{3}\omega_0) + R^{other} \quad (8)$$

$$R_2 = C[\frac{2}{3}J(0) + \frac{1}{6}J(\omega_0^{'} - \omega_0^{'}) + J(2\omega_0^{'}) + \frac{3}{2}J(\omega_0^{'})] + R^{other} \quad (9)$$

$$R_{1\rho} = C[\frac{2}{3}J(2\omega_1) + \frac{1}{6}J(\omega_0^{'} - \omega_0^{'}) + J(2\omega_0^{'}) + \frac{3}{2}J(\omega_0^{'})] + R^{other} \quad (10)$$

The approximation in equation (8) which consists in replacing $4J(2\omega_0) + J(\omega_0)$ by $5J(\sqrt{3}\omega_0)$ has been shown to be very appropriate [21]. The somewhat complicated expressions of R_2 and $R_{1\rho}$ are due to the existence, in a two-spin system, of a two-quanta coherence (hence the spectral densities at $2\omega_0$ or $2\omega_0^{'}$) and a zero-quantum coherence (emphasized here by $J(\omega_0^{'} - \omega_0^{'})$ which has not the same physical meaning as $J(0)$). There are some important differences with respect to the random field mechanism: $J(0)$ in R_2 becomes $J(2\omega_1)$ in $R_{1\rho}$ while R_1 depends on $J(\sqrt{3}\omega_0)$. This means that the procedure described in the previous section can be applied with a multiplicative factor of 15/2 (in place of 2) and provided that the frequency scale is adapted to each parameter: $\omega = \sqrt{3}\omega_0$ for $R_1(\omega)$ and $\omega = 2\omega_1$ for $R_{1\rho}(\omega)$.

3. Experimental

Two systems presently under investigation in this laboratory, with the objective of obtaining full dispersion curves, *i.e.* from zero up to several hundreds of MHz, were retained for the present study. However, as we are concerned here with the very beginning of the dispersion curve, we shall focus only on the frequency range 0-10 MHz. The first one is the solvent (toluene) necessary to the formation of an organogel built with a modified amino-acid [22]; the problem is to know whether, once the gel is formed, toluene still interacts with its surface (experiments performed at 20°C). An unexpected complication occurs due to dissolved oxygen in pure toluene, providing a strong paramagnetic contribution to relaxation rates [23]. At the time the organogel was prepared, we were not aware of this problem which would anyway be difficult to overcome due to the actual preparation procedure. Fortunately, this paramagnetic contribution is constant at low frequencies and can be simply subtracted thus permitting to examine unambiguously the effects of the toluene-gel interaction. On the other hand, due to the number of interacting protons and because it is the total proton magnetization of toluene which is measured, a random field mechanism can be predicted.

The second system is water within a mesoporous medium. In that case, one could wonder if the dipolar relaxation mechanism is intramolecular (the like spins model would prevail) or intermolecular or both. As further discussed in the conclusion, a random field mechanism will be shown to constitute a good approximation for the two latter cases. Anyway, the problem is to characterize, on the one hand, water inside pores, which presumably manifests itself at low frequencies due to a long correlation time, and, on the other hand, interstitial water, which is expected to contribute predominantly at high frequencies due to a smaller correlation time (experiments performed at 25°C). However, for such a system, the whole dispersion curve must be considered and its behavior at very low frequencies can be important for its global analysis.

Proton longitudinal relaxation times were first measured with a Stelar (Mede, Italy) Smartracer relaxometer operating between 5 kHz and 10 MHz according to field cycling automatic procedures [24]. This instrument requires 10 mm o.d. NMR sample tubes which were therefore utilized for subsequent measurements (so as to investigate the very same sample). A home-made spectrometer operating at 200 MHz was employed for $T_{1\rho}$ and T_2 measurements. A special probe, accommodating 10 mm o.d. sample tubes (see above) and capable of handling relatively high rf power for a relatively long time (spin lock periods), was specially constructed. It involves a saddle-shaped coil of 29 mm height and 14.5 mm diameter (silver coated copper wire of 1.5 mm diameter) for covering a substantial portion of the sample with a homogeneous rf field, and high voltage 0.8-10 pF variable non magnetic capacitors (RP series, Polyflon, Norwalk, CT). Its quality factor is of 470. As a matter of fact, problems were encountered, not with the probe but with the stability and possible droops of the power amplifier. This prevents to go beyond 13 kHz (the rf field amplitude being expressed in frequency units) with durations of the spin-lock period up to 6s. This seemingly modest performance (as compared to a previous probe designed for 5mm o.d. sample tubes [25]) is due to the unfavorable coil geometry adapted to the 10mm o.d. sample tubes.

$T_{1\rho}$ was deduced from the decay of the locked magnetization [19,20] under on-resonance conditions, implying two distinct experiments in the case of toluene, one for the methyl and the other for the aromatic resonances. The spin locking field amplitude is varied from experiment to the other and calibrated from the duration of a 180° rf pulse. T_2 was measured according to the CPMG method [26] in order to compensate imperfections of the 180° rf pulses and with a sufficient number of pulses in order to reduce diffusion effects, which, due to background gradients, could be important in the case of porous media [1].

4. Results and discussion

Figure 1 shows toluene raw data in the range 1 kHz-10 MHz ($R_{1\rho}$, R_1) for the pure solvent and for the solvent in the organogel phase. In both cases, one observes, as expected, a plateau at very low frequencies in accord with the first part of a Lorentzian curve (see eq. (1)). In the case of pure toluene, this plateau extends beyond 10 MHz and is attributable to paramagnetic relaxation [23]. Conversely, in the gel phase, the rise beneath 10 MHz is characteristic of a hindered motion, attributable to the interaction with the organogel. The rescaling of $R_{1\rho}$ data against R_1 data has been carried out as explained in the theory section according to the random field model. This is shown in figure 2. Owing to these excellent results, it was deemed unnecessary to try the other model (like spins). On the other hand, T_2 could actually be measured for the methyl resonance but not for the aromatic resonance because of the echo modulation by spin-spin couplings. Thus, the determination of the global R_2 turned out to be impossible. This was not considered as a penalty since $R_{1\rho}$ data just confirm the plateau guessed from R_1 data.

The other system dealt with in this study is water in a mesoporous medium [27]. Figure 3 shows the raw R_1 and $R_{1\rho}$ data obtained at 25° C. In figure 4, the $R_{1\rho}$ data have been rescaled according to the random field model so as to coincide with R_1 data in the overlap region. The consistency of both sets of data is seen to be excellent. Conversely, an attempt to rescale $R_{1\rho}$ data according to the like spins model (see above) is seen to fail (figure 5). Moreover, as shown in figure 6, R_2 appears to be in perfect agreement with what should be $R_{1\rho}$ at zero frequency (see equations (3) and (4)). This demonstrates the consistency of all relaxation data (R_1, $R_{1\rho}$ and R_2). For this system, we have therefore at hand the whole dispersion curve from zero frequency up to several hundreds of MHz (not shown). Indeed, it will be confirmed in a

future work that the data at very low frequencies are essential for properly analyzing dispersion curves.

Conclusion

This study has demonstrated the possibility of obtaining dispersion curves in the whole frequency range, including zero frequency (in the absence of J couplings) and very low frequencies. At least for the two investigated systems (very different in nature), the random field model appears perfectly adequate for linking R_1 and $R_{1\rho}$ evolutions. Besides a change in the frequency scale which is almost the same for R_1 and $R_{1\rho}$ data and, thus, is not very significant, the major difference between the random field model and the like spins model lies in the multiplicative factor which is applied to $R_{1\rho}$ data: 2 for the former model 15/2 for the latter. As a matter of fact, the failure of the like spins model is not very surprising because it applies strictly to a system made of *two* isolated spins, a situation which is rarely encountered. Indeed, it can be shown that this property could be extended to a multi-spin system if and only if all the cross-relaxation rates are identical.

Acknowledgements

We are grateful to Alain Retournard and Pierre-Louis Marande for technical assistance. This work is part of the ANR project “Instrumentation in Magnetic Resonance” (Grant Blan06-2_139020) and also of the ANR project MULOWA (Grant Blan08-1_325450).

The thorough analysis of the manuscript by an anonymous referee and its subsequent improvement are gratefully acknowledged.

References

[1] R. Kimmich, NMR – Tomography, Diffusometry, Relaxometry, Springer, Berlin, 1997.

[2] D.C. Look, I.J. Lowe, J. Chem. Phys. 44 (1966), 2995.

[3] S.W. Kelly, C.A. Sholl, J. Phys.: Condens. Matter 4 (1992), 3317.

[4] R. Kimmich, S. Stapf, M. Möller, R. Out, R.O. Seitter, Macromolecules 27 (1994), 1505.

[5] P.H. Fries, D. Imbert, A. Melchior, J. Chem. Phys. 132 (2010) 044502.

[6] E. Belorizky, D.G. Gillies, W. Gorecki, K. Lang, F. Noack, C. Roux, J. Struppe, L.H. Sutcliffe, J.P. Travers, X. Wu, J. Phys. Chem. A102 (1998), 3674.

[7] E. Anoardo, F. Grinberg, M. Vilfan, R. Kimmich, Chem. Phys. 297 (2004), 99.

[8] E. Anoardo, C. Hauser, R. Kimmich, J. Magn. Reson. 142 (2000), 372.

[9] T. Szyperski, P. Luginbühl, G. Otting, P. Güntert, K. Wüthrich, J. Biomol. NMR 3 (1993), 151.

[10] M. Akke, A.G. Palmer III, J. Am. Chem. Soc. 118 (1996), 911.

[11] S. Zinn-Justin, P. Berthault, M. Guenneugues, H. Desvaux, J. Biomol. NMR 10 (1997), 363.

[12] M. Akke, J. Liu, J. Cavanagh, H.P. Erickson, A.G. Palmer III, Nat. Struct. Biol. 5 (1998), 55.

[13] F.A.A. Mulder, P.J.A. van Tilborg, R. Kaptein, R. Boelens, J. Biomol. NMR 13 (1999), 275.

[14] D.M. Korzhnev, V.Yu. Orekov, F.W. Dahlquist, L.E. Kay, J. Biomol. NMR 26 (2003), 39.

[15] C. Eichmüller, N.R. Skrynnikov, J. Biomol. NMR 32 (2005), 281.

[16] H. Desvaux, N. Birlirakis, C. Wary, P. Berthault, Mol. Phys. 86 (1995), 1059

[17] A. Abragam, The Principles of Nuclear Magnetism, Clarendon Press, Oxford, 1961.

[18] E. Belorizky, P.H.Fries, L. Helm, J. Kowalewski, D. Kruk, R.R. Sharp, P.-O. Westlund, J. Chem. Phys. 128 (2008), 052315.

[19] J. Kowalewski, L. Mäler, Nuclear Spin Relaxation in Liquids: Theory, Experiments and Applications, Taylor & Francis, London, 2006

[20] D. Canet, Nuclear Magnetic Resonance: Concepts and Methods, Wiley, Chichester, 1996.

[21] S.H. Koenig, W.E. Schillinger, J.Biol. Chem. 244 (1969), 3283.

[22] Q.N. Pham, N. Brosse, D. Dumas, A. Hocquet, B. Jamart-Grégoire, New J. Chem. 32 (2008), 1131.

[23] M. Yemloul, S. Bouguet-Bonnet, E. Steiner, A. Robert, F. Allix, B. Jamart-Grégoire, D. Canet, Langmuir, submitted.

[24] R. Kimmich, E. Anoardo, Prog. Nucl. Magn. Reson. Spectrosc. 44 (2004), 257.

[25] H. Chaumette, D. Grandclaude, P. Tekely, D. Canet, C. Cardinet, A. Verschave, J. Phys. Chem. A105 (2001), 8850.

[26] S. Meiboom, D. Gill, Rev. Sci. Instrum. 29 (1958), 688.

[27] J.L. Blin, P. Lesieur; M.J. Stébé, Langmuir 20 (2004) 491.

Figure captions

Figure 1. Raw data of pure Toluene (20° C). Filled triangles: R_1. Open triangles : $R_{1\rho}$.
Raw data of Toluene in the organogel phase (20° C). Filled squares: R_1. Open squares : $R_{1\rho}$.

Figure 2. Filled squares: R_1 data of Toluene in the organogel phase (20° C, identical to fig. 1). Open squares : $R_{1\rho}$ data rescaled for coinciding with R_1 data in the overlap region (see text).

Figure 3. Raw data for water in a porous medium (25°C). Filled squares: R_1. Open squares: $R_{1\rho}$.

Figure 4. Filled squares: R_1 data of water in a porous medium (25° C, identical to fig. 3). Open squares : $R_{1\rho}$ data rescaled for coinciding with R_1 data in the overlap region (according to the random field model, see text).

Figure 5. Same as figure 4 but with the like spins model showing the inadequacy of the model. Note the modifications of the frequency scales according to the procedure detailed in the text.

Figure 6. Same as figure 1 with normal ordinate and abscissa scales (and reduced frequency range) permitting to display the R_2 value (triangle at zero frequency).

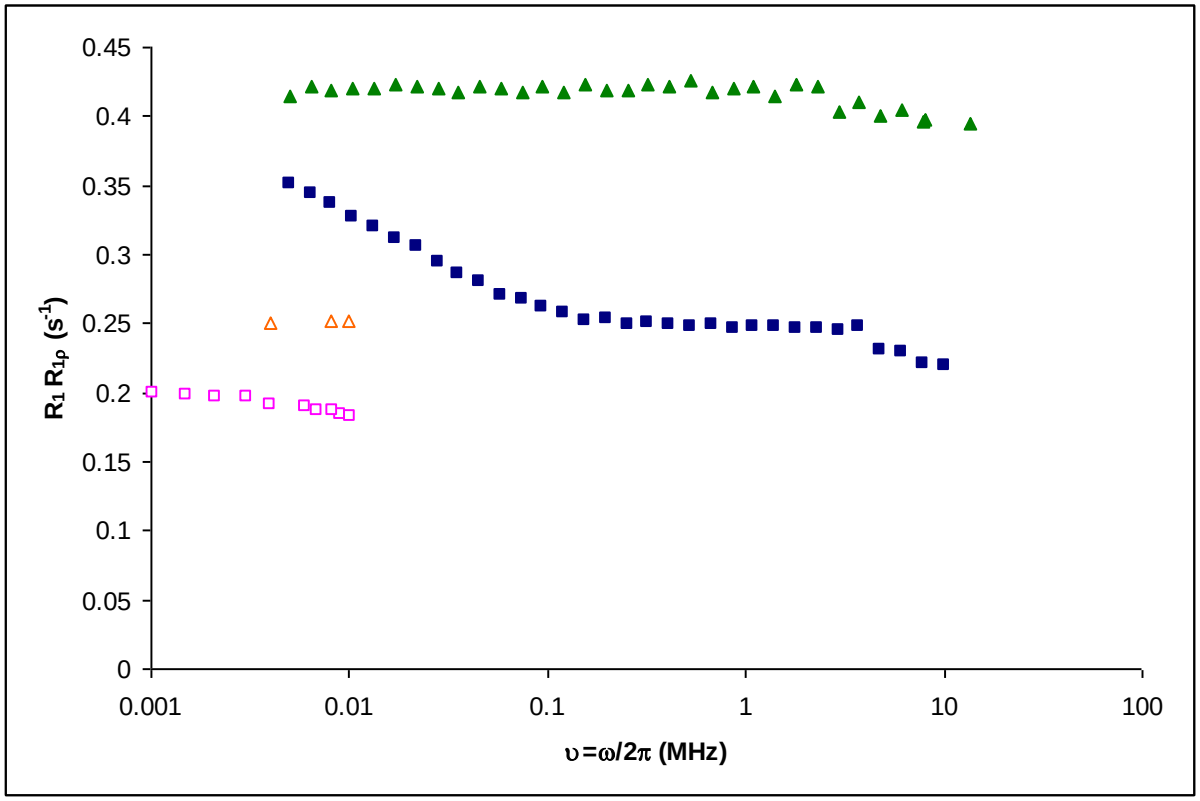
0.45
0.4
0.35
0.3
0.25
0.2
0.15
0.1
0.05
0
R1 R1ρ (s-1)
0.001
0.01
0.1
1
10
100
υ=ω/2π (MHz)

Figure 1

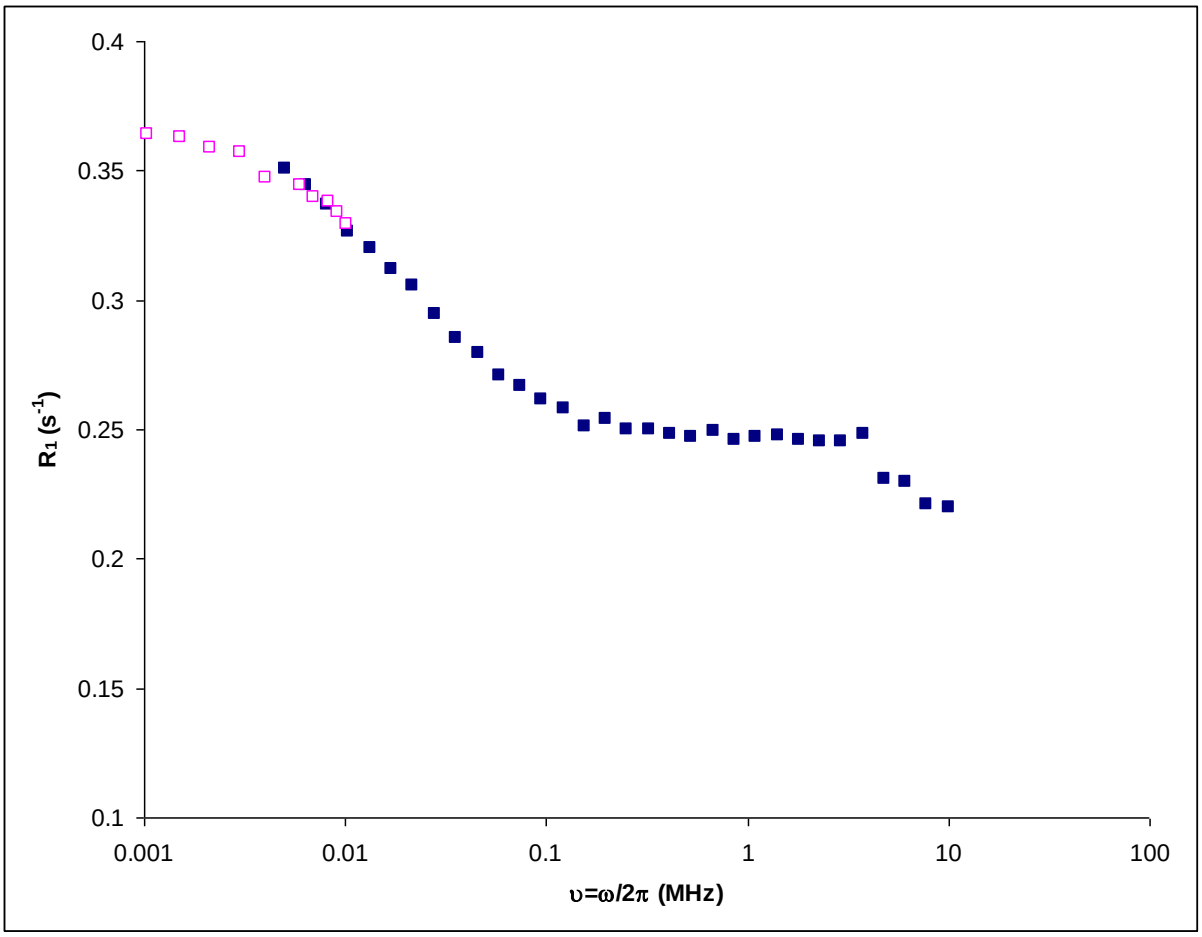

Figure 2

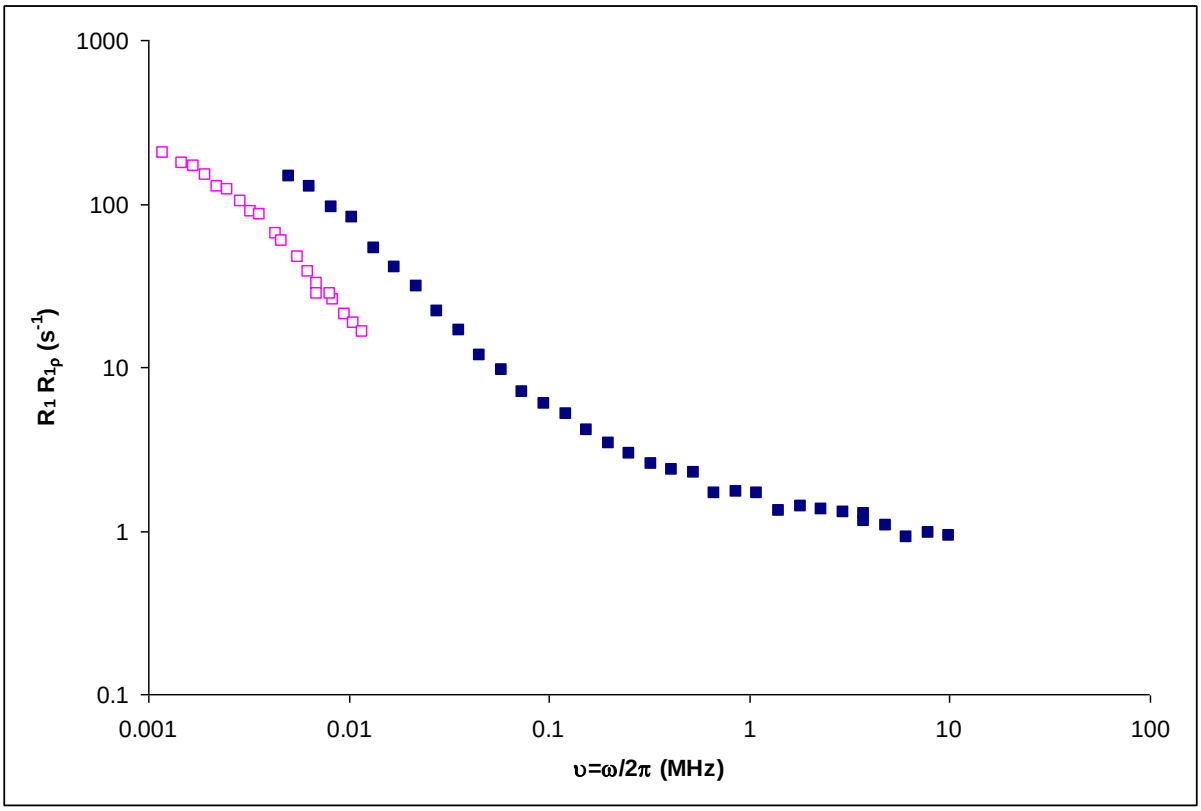

Figure 3

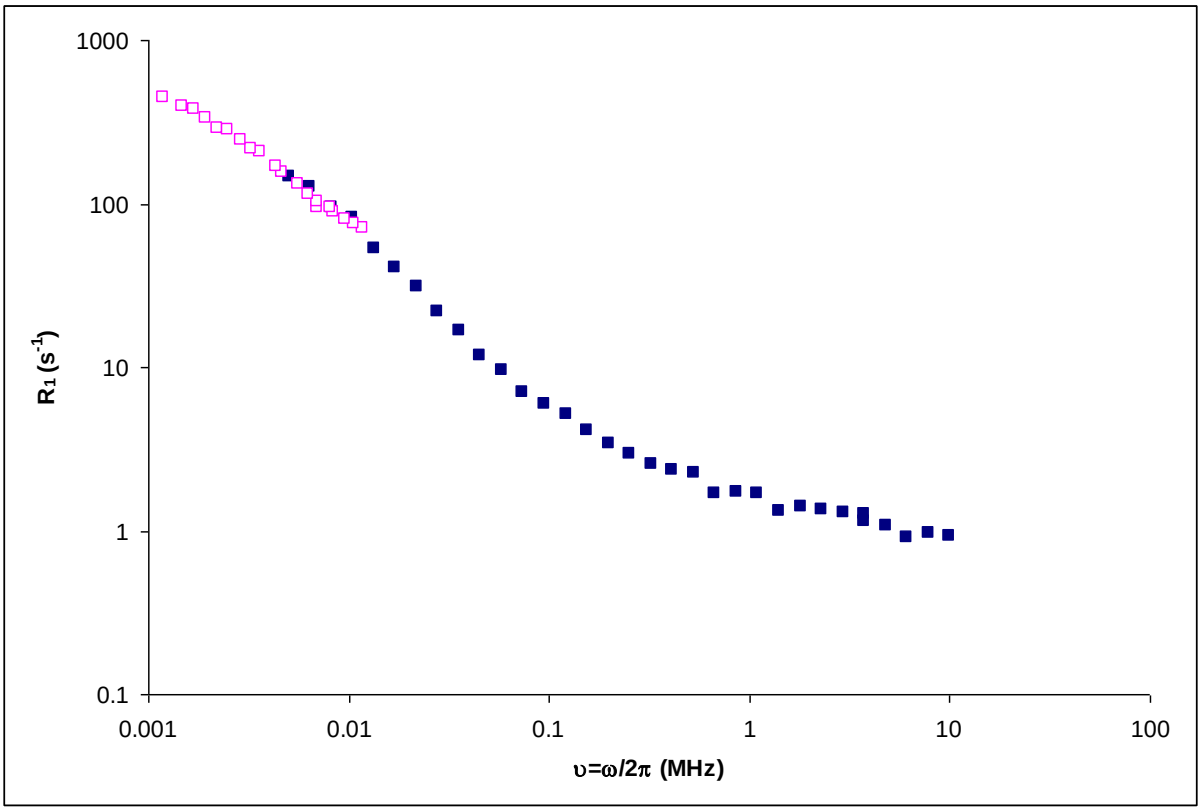

Figure 4

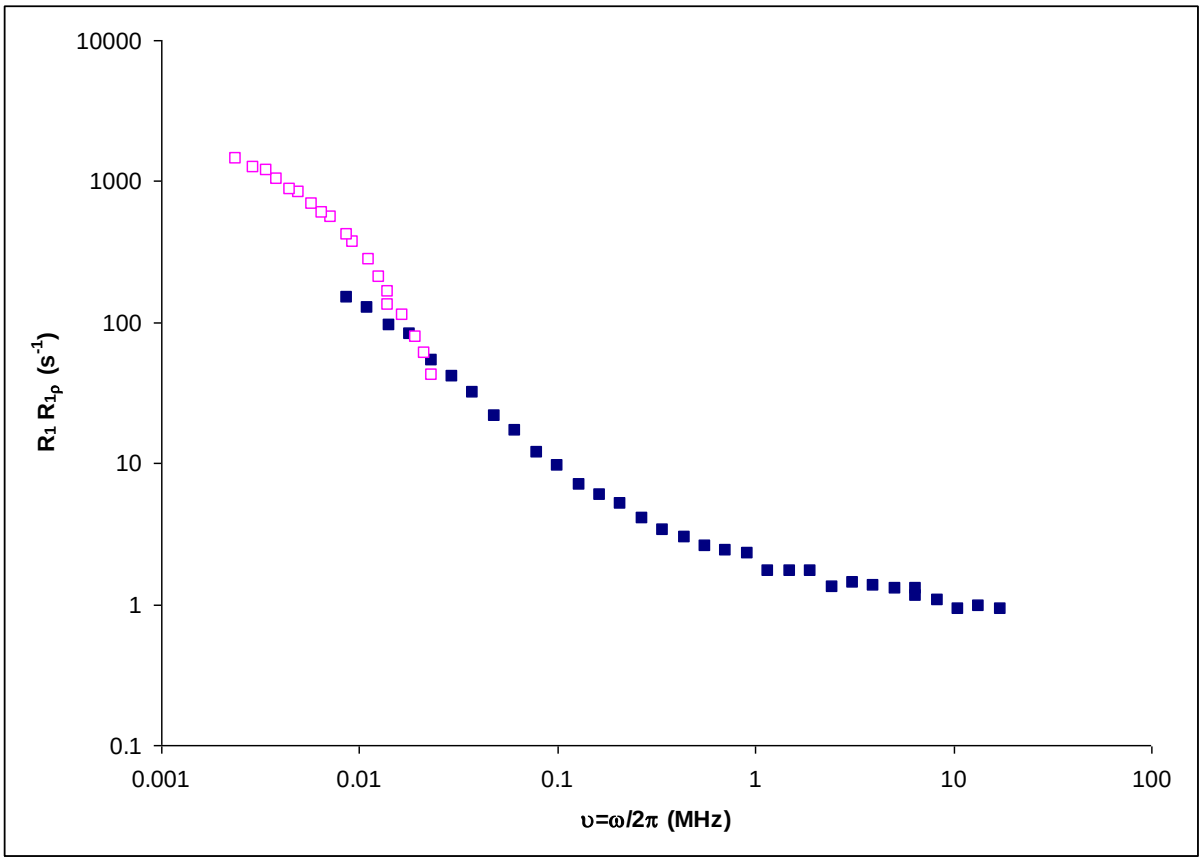

Figure 5

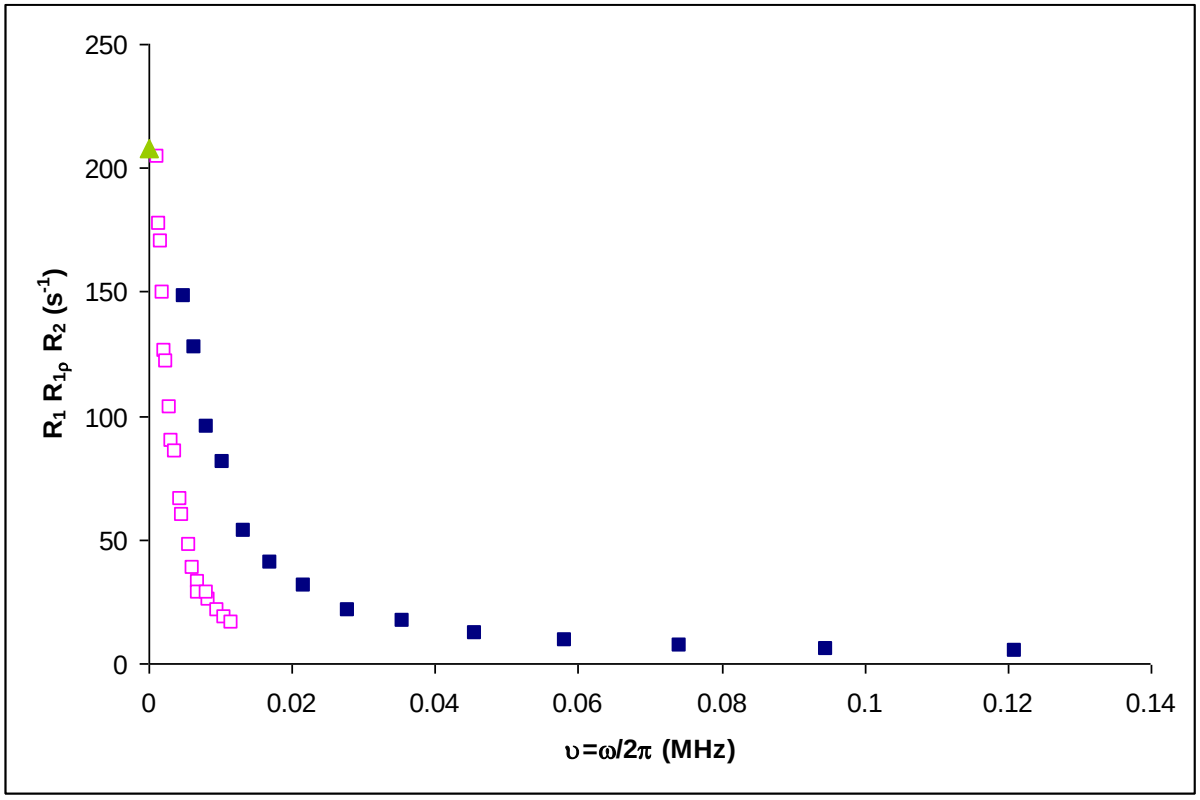
250
200
150
100
50
0
0
0.02
0.04
0.06
0.08
0.1
0.12
0.14
R1 R1ρ R2 (s-1)
υ=ω/2π (MHz)

Figure 6